



2-{2,6-Bis[bis(4-fluorophenyl)methyl]-4-chlorophenylimino}-3-aryliminobutynickel(II) bromide complexes: Synthesis, characterization, and investigation of their catalytic behavior

Qingyun Liu^{a,b}, Wenjuan Zhang^b, Dedong Jia^b, Xiang Hao^b,
Carl Redshaw^{c,*}, Wen-Hua Sun^b

^a College of Chemistry and Environmental Engineering, Yangtze University, Hubei, Jingzhou 434023, China

^b Key Laboratory of Engineering Plastics and Beijing National Laboratory for Molecular Sciences, Institute of Chemistry, Chinese Academy of Sciences, Beijing 100190, China

^c Department of Chemistry, University of Hull, Hull HU6 7RX, UK



ARTICLE INFO

Article history:

Received 16 November 2013

Received in revised form 13 January 2014

Accepted 16 January 2014

Available online 24 January 2014

Keywords:

α -Diiminonickel complex
bulky unsymmetrical 2,3-diiminobutane
ethylene polymerization
highly branched polyethylene

ABSTRACT

The series of 2-{2,6-bis[di(4-fluorophenyl)methyl]-4-chlorophenylimino}-3-aryliminobutane derivatives (**L1–L5**) and their nickel(II) dibromide complexes (**Ni1–Ni5**) were synthesized, and all organic compounds were fully characterized by the Fourier transform infrared (FT-IR) and nuclear magnetic resonance (NMR) spectroscopy and by elemental analysis, while the nickel complexes were characterized by FT-IR spectroscopy, elemental analysis, as well as by single-crystal X-ray diffraction for two representative examples, namely **Ni1** and **Ni4**. A distorted tetrahedral geometry was observed for these four-coordinate nickel complexes. Upon the activation with either Methylaluminoxane or modified methylaluminoxane as co-catalyst, all nickel complex precatalysts showed very high activity toward ethylene polymerization with activities of up to 10^7 g(PE)-mol⁻¹(Ni)-h⁻¹, and afforded highly branched polyethylene with a bimodal distribution.

© 2014 Elsevier B.V. All rights reserved.

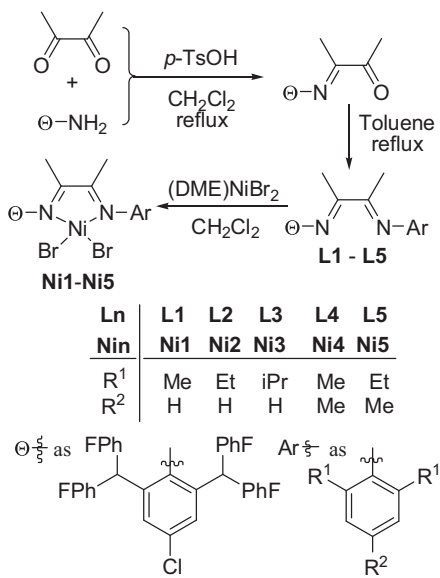
1. Introduction

The discovery of α -diimine nickel(II) and Pd(II) complexes as highly active precatalysts resurrected interest in late-transition metal based systems for possible polyolefin production [1–3]. Extensive modification of the complex precatalysts and exploration of their catalytic behavior as well as the properties of the resulting polyethylene has been well documented by several review articles [4–8] and more recent papers on iminopyridyl-nickel pre-catalysts have also appeared [9–11]. The steric bulk of the modified ligands can play an important role in determining the catalytic behavior of their nickel complexes. For example, the use of less bulky ligands can transform their nickel precatalysts in such a way that results in more oligomers due to enhanced chain transfer versus chain propagation [3,12,13]; whereas the use of bulkier ligands aids the formation of highly branched polyethylene [12]. In addition, unsymmetrical α -diiminonickel(II) complex

precatalysts, potentially having *meso*- and *rac*-stereo isomers, can produce polyethylene with broad polydispersity or a bimodal distribution [12]. Interestingly, benzhydryl-substituted unsymmetrical acenaphthyl-diiminonickel complexes not only exhibited very high activity toward ethylene polymerization, but also produced highly branched polyethylene with a unimodal feature [14–16]. Subsequently, butane-based unsymmetrical diiminonickel complexes were shown to produce polyethylene with broad polydispersity [17], while benzhydryl-substituted butane-based symmetrical diiminonickel complexes were confirmed to possess high activity toward ethylene polymerization [18]. Furthermore, the use of a fluoro-substituent has been recognized to have a positive influence on the catalytic behavior of their metal complexes, and can result in living polymerization [19] and/or better thermal stability [20]. Furthermore, our previous experience has revealed a number of positive effects using iron complex precatalysts bearing this type of ligand set in ethylene polymerization [21,22]. In order to extend the scope of butane-based unsymmetrical diiminonickel complexes available [17], the synthesis of 2-{2,6-bis[di(4-fluorophenyl)methyl]-4-chlorophenylimino}-3-aryliminobutane derivatives (**L1–L5**) and

* Corresponding author: Tel.: +44 1482 465219; fax: +44 1482 466410.

E-mail address: c.redshaw@hull.ac.uk (C. Redshaw).



Scheme 1. Synthesis of diiminobutanes **L1–L5** and nickel complexes **Ni1–Ni5**.

the corresponding nickel(II) (**Ni1–Ni5**) complexes has now been carried out, and investigations into the catalytic behavior of the nickel complexes have been conducted. Upon activation with either Methylaluminoxane (MAO) or modified methylaluminoxane (MMAO), all nickel complexes performed with very high activity toward ethylene polymerization, producing polyethylene with a bimodal distribution.

2. Experiments

2.1. General

All manipulations of air- and moisture-sensitive compounds were carried out under an atmosphere of nitrogen using standard Schlenk techniques. Toluene was dried by refluxing with sodium and distilled under nitrogen prior to use. MAO, 1.46 M solution in toluene and MMAO, 1.93 M in heptane, 3 Å, were purchased from Akzo Nobel Corp. High-purity ethylene was purchased from Beijing Yanshan Petrochemical Co. and used as received. ¹H and ¹³C NMR spectra were recorded on a Bruker DMX 400 MHz instrument at ambient temperature using tetramethylsilane (TMS) as an internal standard. IR spectra were recorded on a Perkin-Elmer System 2000 FT-IR spectrometer. Elemental analyses were carried out using a Flash EA 1112 microanalyzer. Molecular weights (M_w) and molecular weight distribution (M_w/M_n) of polyethylene were determined by a PL-GPC220 at 150 °C, with 1,2,4-trichlorobenzene as the solvent. Differential scanning calorimetric (DSC) traces and melting points of polyethylene were obtained from the second scanning run on Perkin-Elmer DSC-7 at a heating rate of 10 °C/min. ¹³C NMR spectra of polymer were recorded on a Bruker DMX-300 MHz instrument at 135 °C in deuterated 1,2-dichlorobenzene with TMS as an internal standard.

2.2. Syntheses and characterization

The organic compounds to be used as the ligands were prepared according to the modified literature procedure [17], and the resulting diimino compounds were reacted with nickel bromide in dichloromethane to afford the corresponding nickel complexes; the synthetic procedure is illustrated in **Scheme 1**. The detailed protocol of the synthesis of diimino compounds (**L1–L5**) is available in the Supplementary information.

2.2.1. Synthesis of nickel complexes (**Ni1–Ni5**)

According to our previous procedure [17], the complexes **Ni1–Ni5** were prepared by the reaction of (DME)NiBr₂ with the corresponding ligand (**L1–L5**) in dichloromethane. The procedure for **Ni1** is as follows. The ligand **L1** (0.1 g, 0.14 mmol) and (DME)NiBr₂ (0.05 g, 0.16 mmol) were added to a Schlenk tube together with 10 ml of dichloromethane. The reaction mixture was stirred for 12 h at room temperature, and diethyl ether (10 ml) was added to precipitate the complex. The precipitate was washed with diethyl ether and dried under vacuum to afford a brick red powder of **Ni1** in 87.8% (0.12 g) yield. FT-IR (KBr, cm⁻¹): 3058 (w), 2168 (w), 1899 (w), 1602 (m), 1506 (s), 1436 (m), 1377 (m), 1225 (s), 1158 (s), 1098 (m), 1012 (m), 983 (w), 907 (w), 832 (s), 793 (m), 721 (m), 668 (m). Analytical Calculated (Anal. Calcd.) for C₄₄H₃₅Br₂ClF₄N₂Ni (921.71): C, 57.34; H, 3.83; N, 3.04. Found: C, 56.91; H, 4.16; N, 2.93.

Data for **Ni2**. Yield: 85.0% (0.11 g), brick red powder. FT-IR (KBr, cm⁻¹): 3052 (w), 2043 (w), 1601 (m), 1577 (m), 1504 (s), 1437 (m), 1408 (m), 1377 (s), 1298 (w), 1212 (s), 1156 (s), 1096 (m), 1038 (w), 1012 (w), 995 (m), 903 (m), 831 (s), 764 (m), 668 (m). Anal. Calcd. for C₄₆H₃₉Br₂ClF₄N₂Ni (949.76): C, 58.17; H, 4.14; N, 2.95. Found: C, 58.11; H, 4.53; N, 2.91.

Data for **Ni3**. Yield: 92.9% (0.12 g), brick red powder. FT-IR (KBr, cm⁻¹): 3052 (w), 2967 (m), 2166 (w), 1600 (m), 1578 (w), 1505 (s), 1439 (m), 1413 (w), 1378 (s), 1204 (m), 1158 (s), 1097 (m), 1054 (w), 1008 (w), 911 (m), 836 (s), 794 (m), 735 (m), 669 (m). Anal. Calcd. for C₄₈H₄₃Br₂ClF₄N₂Ni (977.82): C, 58.96; H, 4.43; N, 2.86. Found: C, 58.57; H, 4.48; N, 2.93.

Data for **Ni4**. Yield: 86.6% (0.11 g), brick red powder. FT-IR (KBr, cm⁻¹): 3043 (w), 2910 (w), 2168 (w), 2043 (w), 1599 (m), 1576 (m), 1504 (s), 1437 (m), 1408 (m), 1377 (s), 1297 (w), 1219 (s), 1156 (s), 1096 (m), 1011 (m), 983 (w), 907 (m), 831 (s), 713 (w), 668 (m). Anal. Calcd. for C₄₅H₃₇Br₂ClF₄N₂Ni (935.74): C, 57.76; H, 3.99; N, 2.99. Found: C, 57.78; H, 4.36; N, 2.87.

Data for **Ni5**. Yield: 92.5% (0.12 g), brick red powder. FT-IR (KBr, cm⁻¹): 2967 (m), 2168 (m), 2043 (w), 1600 (m), 1576 (w), 1504 (s), 1438 (w), 1414 (w), 1379 (m), 1335 (w), 1301 (w), 1221 (s), 1157 (s), 1096 (m), 1011 (w), 984 (w), 911 (m), 832 (s), 721 (m), 669 (m). Anal. Calcd. for C₄₇H₄₁Br₂ClF₄N₂Ni (963.79): C, 58.57; H, 4.29; N, 2.91. Found: C, 58.77; H, 4.23; N, 2.89.

2.2.2. X-Ray crystallographic studies

Single crystals of complexes **Ni1** and **Ni4** suitable for X-ray diffraction were grown by slow diffusion of diethyl ether into the respective dichloromethane solution. Data collection of **Ni1** and **Ni4** was performed with a Rigaku R-AXIS Rapid IP diffractometer with graphite-monochromated Mo K α radiation ($\lambda = 0.71073 \text{ \AA}$) at 173(2) K. Intensities were corrected for Lorentz and polarization effects and empirical absorption. The structures were solved by direct methods and refined by full-matrix least squares on F^2 . All hydrogen atoms were placed in calculated positions. Structure solution and refinement were performed using the SHELXL-97 package [23]. Crystal data and processing parameters for complexes **Ni1** and **Ni4** are summarized in **Table 1**.

2.3. General procedure for ethylene polymerization

2.3.1. Ethylene polymerization at 1 atmosphere (atm) ethylene pressure

The precatalyst **Ni1** was dissolved in toluene in a Schlenk tube, and then the reaction solution was stirred with a magnetic stir bar at 1 atm of ethylene at the required reaction temperature. The required amount of cocatalyst was added by a syringe. After the requisite time, the reaction solution was quenched with 10% hydrochloric acid in ethanol. The precipitated polymer was collected by

Table 1
Crystal data and structure refinement for **Ni1** and **Ni4**.

	Ni1	Ni4
Empirical formula	C ₄₄ H ₃₅ Br ₂ ClF ₄ N ₂ Ni	C ₄₅ H ₃₇ Br ₂ ClF ₄ N ₂ Ni
Fw	921.72	935.75
T/K	173(2)	173(2)
$\lambda/\text{\AA}$	0.71073	0.71073
Cryst. syst.	Monoclinic	Monoclinic
Space group	Cc	Cc
$a/\text{\AA}$	24.466(5)	24.183(5)
$b/\text{\AA}$	11.099(2)	11.066(2)
$c/\text{\AA}$	16.588(3)	16.655(3)
$\alpha (\text{°})$	90	90
$\beta (\text{°})$	121.07(3)	117.48(3)
$\gamma (\text{°})$	90	90
V (\AA^3)	3858.5(13)	3954.0(14)
Z	4	4
D calcd. (g cm^{-3})	1.587	1.572
μ/mm^{-1}	2.698	2.634
F(000)	1856	1888
Cryst. size/mm	0.24 × 0.21 × 0.05	0.19 × 0.16 × 0.03
θ range (°)	2.79–27.48	1.90–27.50
Limiting indices	-31 ≤ h ≤ 31 -14 ≤ k ≤ 14 -21 ≤ l ≤ 21	-31 ≤ h ≤ 31 -14 ≤ k ≤ 14 -21 ≤ l ≤ 21
No. of reflections collected	14124	13010
No. unique reflections [$R(\text{int})$]	8072 (0.0604)	7865 (0.0438)
Completeness to θ (%)	99.4%	98.9%
Absorption correction	none	none
Data/restraints/parameters	8072/2/487	7865/2/496
Goodness of fit on F^2	1.057	1.089
Final R indices [$I > 2\sigma(I)$]	$R_1 = 0.0823$ $wR_2 = 0.2050$	$R_1 = 0.0868$ $wR_2 = 0.2263$
R indices (all data)	$R_1 = 0.0890$ $wR_2 = 0.2131$	$R_1 = 0.1005$ $wR_2 = 0.2553$
Largest diff. peak and hole (e \AA^{-3})	0.917 and -0.659	1.045 and -0.964

filtration, washed with ethanol several times, and dried in a vacuum at 60 °C until constant weight.

2.3.2. Ethylene polymerization at 10/5 atm ethylene pressure

The polymerization at 10 atm of ethylene pressure was performed in a 250 mL stainless steel autoclave equipped with a mechanical stirrer, a temperature controller, and gas ballast through a solenoid valve for continuous feeding of ethylene at constant pressure. First, 30 mL of toluene was injected into the autoclave, which has previously been filled with ethylene. When the temperature required was reached, another 20 mL toluene containing the dissolved complex was added, plus the required amount of co-catalyst (MAO or MMAO), and the remaining toluene were successively added using a syringe. The reaction mixture was intensively stirred for the desired time under the corresponding pressure of ethylene throughout the entire experiment. The reaction was terminated and analyzed using the same method as above for ethylene polymerization at ambient pressure.

3. Results and Discussion

3.1. Synthesis, characterization of diiminobutanes and nickel(II) complexes

The synthetic procedure was carried out as previously reported [17], and all organic compounds (**L1–L5**) were fully characterized by ¹H/¹³C NMR and FT-IR spectroscopy as well as by elemental analysis. Treatment of the compounds **L1–L5** with one equivalent of (DME)NiBr₂ afforded the respective nickel bromide complexes (**Ni1–Ni5**) (Scheme 1), which were characterized by FT-IR spectroscopy and elemental analysis. To further confirm their structures, single crystals of **Ni1** and **Ni4** suitable for X-ray

Table 2
Selected bond lengths (Å) and angle (°) for complexes **Ni1** and **Ni4**.

Complexes	Ni1	Ni4
Bond lengths (Å)		
Ni(1)-N(1)	2.026(7)	2.038(7)
Ni(1)-N(2)	2.004(7)	2.004(9)
Ni(1)-Br(1)	2.3276(14)	2.3307(17)
Ni(1)-Br(2)	2.3383(15)	2.3328(16)
N(1)-C(2)	1.301(10)	1.291(14)
N(1)-C(5)	1.421(11)	1.444(13)
N(2)-C(1)	1.282(11)	1.279(13)
N(2)-C(13)	1.459(11)	1.447(14)
C(1)-C(2)	1.500(11)	1.468(15)
Bond angles (°)		
N(1)-Ni(1)-N(2)	80.9(3)	80.8(3)
N(1)-Ni(1)-Br(1)	112.9(2)	111.2(3)
N(1)-Ni(1)-Br(2)	111.7(2)	114.1(3)
N(2)-Ni(1)-Br(1)	118.7(2)	108.0(3)
N(2)-Ni(1)-Br(2)	107.7(2)	116.7(2)
Br(1)-Ni(1)-Br(2)	118.74(6)	119.64(6)

diffraction analysis were obtained, and the crystal structures are shown in Figs. 1 and 2; selected bond lengths and bond angles are tabulated in Table 2.

Similar to our previous report on α -diimino nickel analogues [17], both structures of the complexes **Ni1** and **Ni4** revealed a distorted tetrahedral geometry at the nickel center, for which the atoms of N1, N2, and Br2 comprised the basal plane, and the atom Br1 occupied the apical position. The aryl rings of the α -diimine are almost perpendicular to the coordination plane formed by N1-C2-C1-N1. In the structure of complex **Ni1** (shown in Fig. 1), the dihedral angle of the coordination plane to the plane formed by C13, C14, C18 and to the plane formed by C5, C6, C10 are 86.91° and 88.97°, respectively, while the respective values in **Ni4** are 86.60° and 88.56°, which are slightly larger than for the analog without the fluoro-substituent [17]. The bond lengths of Ni-N [2.026(7) and 2.004(7) Å for **Ni1** (2.038(7) and 2.003(9) Å for **Ni4**] are much longer than those reported for the nickel analogs minus the fluoro-substituent [2.012(4), 1.999(4) Å for **Ni4'**, 2.002(5) and 1.989(6) Å for **Ni5'**]; this is ascribed to fluoro-incorporation leading to an electron-deficient nickel center. According to the data in Table 2, the complexes **Ni1** and **Ni4** have similar structural features, and therefore the complex **Ni4** is not further discussed.

3.2. Ethylene polymerization

Using **Ni2** as precatalysts, the ethylene polymerization was evaluated in the presence of different co-catalysts such as MAO, MMAO, and Et₂AlCl. The cocatalysts MAO or MMAO showed high efficiency in the ethylene polymerization, which is consistent with the observation found for other nickel precatalysts [17], and therefore investigations were conducted by employing either MAO or MMAO as cocatalyst.

3.2.1. Ethylene polymerization by the **Ni1–Ni5/MAO** systems

In the presence of MAO, precatalyst **Ni2** was employed for optimizing the ethylene polymerization conditions and the results are collected in Table 3. At 20 °C, increasing the Al/Ni ratio from 1000 to 3000 led to little change of polymerization activity, which range from 3.84 to $4.53 \times 10^6 \text{ g mol}^{-1}(\text{Ni}) \text{ h}^{-1}$ (runs 1–5, Table 3), while the highest activity was achieved at a molar ratio of Al/Ni 2000:1; this is similar to that found for the analog **Ni2'/MAO** [14]. In contrast, the molecular weights of the obtained polyethylenes decreased from 10.7 to $6.73 \times 10^5 \text{ g mol}^{-1}$ along with higher Al/Ni ratios, indicating that more chain transfer to aluminum occurs at higher concentrations of cocatalyst. The effect of temperature on the activity was also

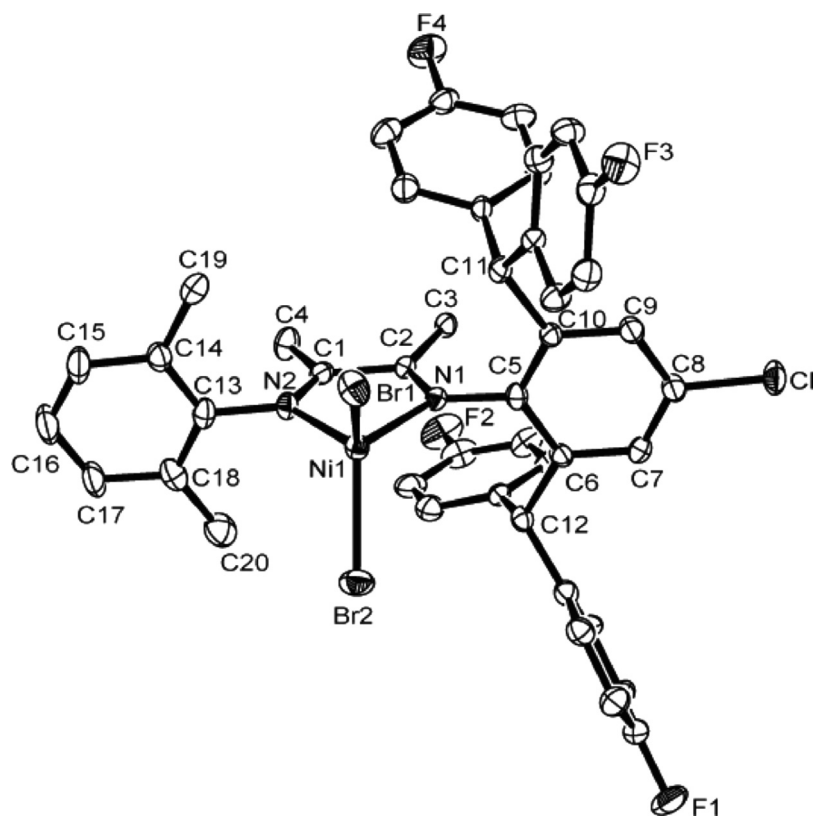


Fig. 1. ORTEP drawing of complex **Ni1** with thermal ellipsoids at 30% probability level. Hydrogen atoms have been omitted for clarity.

investigated at the molar ratio of Al/Ni of 2000:1. On elevating the temperature from 20 °C to 30 °C, the polymerization activity dramatically increased from 4.53 to $8.19 \times 10^6 \text{ g mol}^{-1} (\text{Ni}) \text{ h}^{-1}$, while further increasing the temperature from 30 °C to 60 °C led to a sharp decrease of polymerization activity

from 8.19 to $0.93 \times 10^6 \text{ g mol}^{-1} (\text{Ni}) \text{ h}^{-1}$ (runs 3, 6–9, Table 3), reflecting the poor stability of the nickel intermediate at higher temperatures. As anticipated, the molecular weight of the resultant polyethylene (PE) decreased from $8.76 \times 10^5 \text{ g mol}^{-1}$ on increasing the temperature from 20 °C to 60 °C. At the same

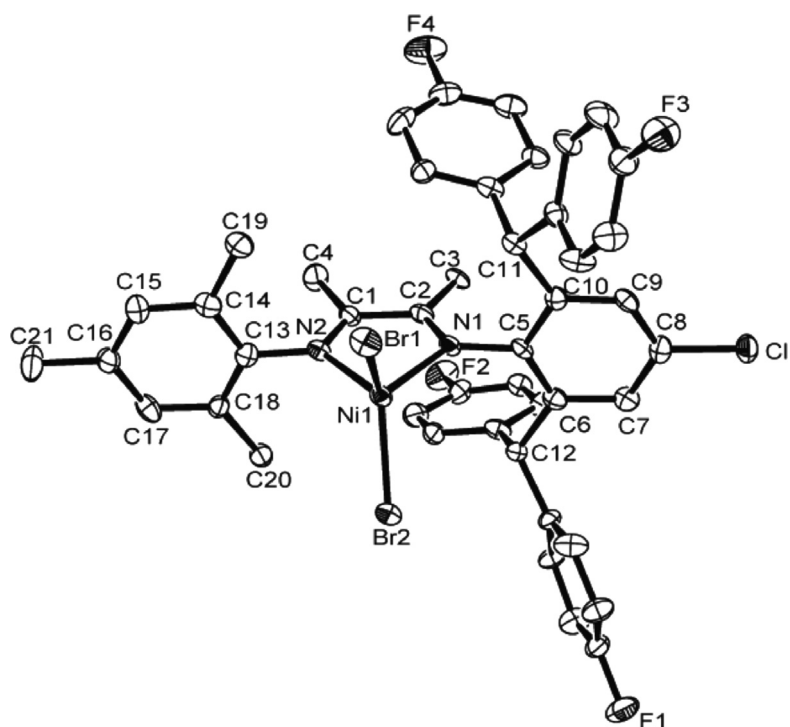


Fig. 2. ORTEP drawing of complex **Ni4** with thermal ellipsoids at 30% probability level. Hydrogen atoms have been omitted for clarity.

Table 3Catalytic Results of Ethylene Polymerization with Ni1–Ni5/MAO^a

run	Cat.	T/°C	t/min	Al/Ni	Activity ^b	M_w^c,d	M_w/M_n^d	$T_m^e(^\circ\text{C})$	Branches ^f
1	Ni2	20	30	1000	3.84	10.7	5.1	97.8	43
2	Ni2	20	30	1500	3.92	9.39	2.3	101.8	49
3	Ni2	20	30	2000	4.53	8.76	2.6	92.5	48
4	Ni2	20	30	2500	3.87	6.73	3.0	72.2	63
5	Ni2	20	30	3000	3.84	—	—	—	—
6	Ni2	30	30	2000	8.19	6.20	3.6	53.9	58
7	Ni2	40	30	2000	2.79	5.91	2.4	44.9	86
8	Ni2	50	30	2000	1.06	4.14	9.7	38.8	89
9	Ni2	60	30	2000	0.93	3.81	7.0	30.6	92
10	Ni2	30	5	2000	11.5	5.26	11.9	58.8	59
11	Ni2	30	10	2000	9.84	4.71	14.7	53.2	82
12	Ni2	30	20	2000	8.72	6.66	17.5	47.1	78
13	Ni2	30	60	2000	6.14	4.92	13.3	51.5	69
14 ^g	Ni2	30	30	2000	2.61	5.44	23.5	58.7	71
15 ^h	Ni2	30	30	2000	0.83	3.01	1.8	31.2	102
16	Ni1	30	30	2000	4.95	7.64	38.3	88.8	77
17	Ni3	30	30	2000	3.81	8.18	51.4	46.5	46
18	Ni4	30	30	2000	4.89	6.34	17.9	52.9	80
19	Ni5	30	30	2000	4.57	6.59	37.8	56.8	60

^a Conditions: 2 μmol Ni; 10 atm of ethylene; 30 min; total volume 100 ml.^b 10⁶ g mol⁻¹(Ni) h⁻¹.^c 10⁶ g mol⁻¹.^d determined by GPC.^e determined by DSC.^f /1000 carbons, determined by FT-IR [26].^g 5 atm of ethylene.^h 1 atm ethylene.

time, higher temperatures also led to a higher branch density for the obtained PE, namely from 48 to 92/1000 carbon. These results can be explained in terms of deactivation of the metal species [1,2,24] and increased chain walking [5,25] at higher temperature. In addition, lower T_m values for the PE were also observed at higher temperature, which agreed with the trend observed for the branch density.

Fig. 3 shows the gel permeation chromatography (GPC) traces of the PE obtained at different temperatures and it reveals that the PE obtained above 20 °C possessed a bimodal distribution and that the fraction for the low molecular weight increased on increasing the temperature. The peaks of the traces also shifted to lower molecular weights, which is similar to the situation observed for Ni2/MAO [17], which is consistent with the formation of more polyethylene of lower molecular weights due to enhanced chain transfer occurring at higher reaction temperatures.

In addition, the ethylene pressure also had an impact on the catalytic performance. For example, increasing the ethylene pressure from 1 to 10 atm led to a huge increase in the activity from 0.83 to 8.91 × 10⁶ g mol⁻¹(Ni) h⁻¹ and a decrease in the branch density from 102 to 58/1000 carbon for the obtained PE (runs 6, 14, 15 in

Table 3). The reason here is the competition between ethylene capture and “chain walking”, which always exists in the polymerization process, with the chain walking being favored at lower pressure leading to higher branching in the polyethylene and the chain propagation favored at higher pressure leading to higher activity and higher molecular weight polymers. On prolonging the reaction time from 5 to 60 min at 30 °C, the catalytic activities gradually decreased from 11.46 to 6.14 × 10⁶ g·mol⁻¹(Ni) h⁻¹, suggesting that the catalytic species remained active over 60 min (run 10–13, Table 3). All the polyethylene obtained possessed a bimodal distribution.

Under the optimized conditions (Al/Ni = 2000, temp. = 30 °C), the ethylene polymerization catalysis of all the nickel complexes Ni1–Ni5 was investigated. In general, all exhibited good activity for ethylene polymerization, affording a bimodal distribution for the polyethylene (shown in Fig. 4) akin to the results using unsymmetrical butene α-diimine complexes, but somewhat different to the unimodal distribution observed for acenaphthylene α-diimine nickel complexes [14–16]; the different conformation of the

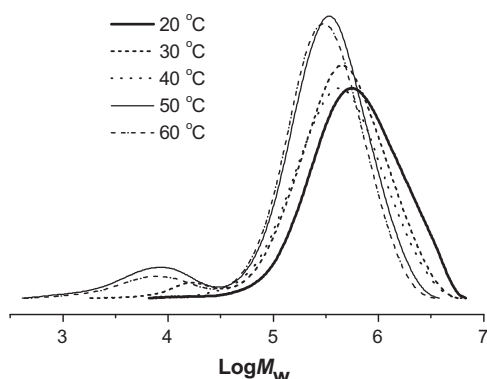


Fig. 3. GPC curves of the polyethylene obtained by Ni2/MAO at different temperatures (runs 3, 6–9 in Table 3).

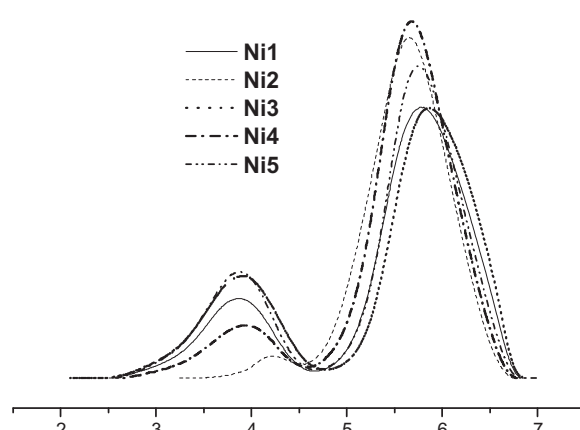


Fig. 4. GPC curves of polyethylene obtained by Ni1–Ni5/MAO (runs 9, 13–16 in Table 3).

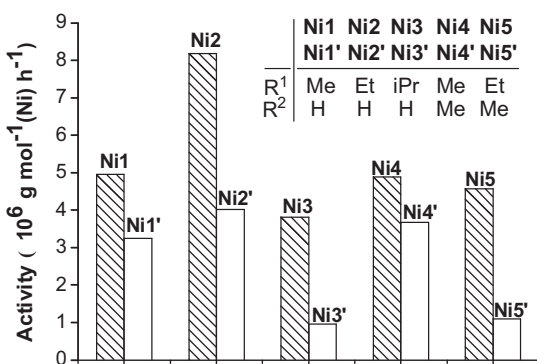


Fig. 5. Comparison of polymerization activities by the **Ni1–Ni5**/MAO with nonfluorinated analogs **Ni1'–Ni5'**/MAO [17].

coordinated ring that favors the generation of two kinds of active species was thought to be the reason.

It is noteworthy that these complexes showed much higher activity than did their analogs without F incorporation (Fig. 5), the reason is attributed to the ability of the electron withdrawing fluoro-substituent present in the ligands of the precatalysts **Ni1–Ni5**, resulting in a higher net charge at the nickel core in comparison to the nonfluorinated analogs **Ni1'–Ni5'**. Indeed, computational studies have revealed that higher catalytic activities are achieved with the enhanced net charges associated with the late-transition metal complex precatalysts [27,28]. Thus, the complex precatalysts **Ni1–Ni5** exhibited much higher activity when compared with their nonfluorinated analogs **Ni1'–Ni5'** [17] (Fig. 5), thereby illustrating the remarkable influence of the ligand fluorine atoms on the activity. In addition, the ligand environment had similar effects on the polymerization behavior to that of previous unsymmetrical α -diimine nickel complexes. According to the data in Table 2, **Ni3** ($R_1 = iPr$) exhibited the lowest activity of all these catalyst systems, however it produced polyethylene with the highest molecular weight (run 14 in Table 3). It is thought that the introduction of the sterically bulky substituents (iPr)

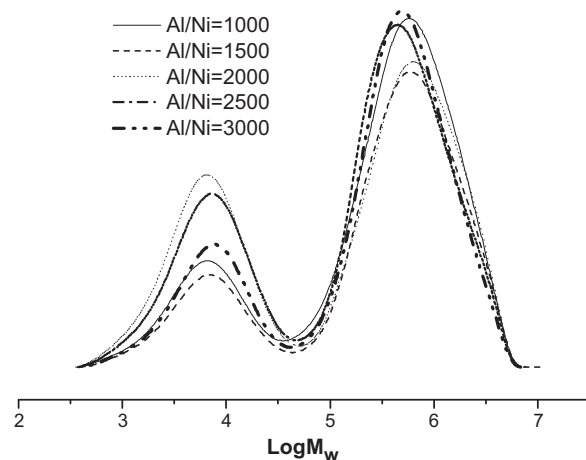


Fig. 6. GPC curves of the polyethylene obtained by **Ni2**/MMAO at different Al/Ni ratios (runs 1–5 in Table 4).

at the *ortho*-positions of the phenyl ring would block the axial sites at the metal center, and can then suppress the chain transfer processes rather than chain propagation [29]. Given that the F position is far removed from the nickel center, we proposed that the electron withdrawing group reduces the electron density at the nickel center which leads to the higher observed activity (rather than any steric effect). In addition, the molecular weights of polyethylenes formed by **Ni1–Ni5** are generally smaller than those by the nonfluorinated **Ni1'–Ni5'** systems [17], besides **Ni3** and its analog **Ni3'** containing the bulkier iPr substituent at the *ortho*-position of the N-aryl.

3.2.2. Ethylene polymerization with the **Ni1–Ni5**/MMAO systems

The above results revealed that the catalytic systems **Ni1–Ni5**/MAO exhibited higher activity than did their analogs **Ni1'–Ni5'**/MAO [17], and produced polymer with a bimodal

Table 4
Catalytic Results of Ethylene Polymerization with **Ni1–Ni5**/MMAO^a.

run	cat. ($R^1 R^2$)	T/°C	t/min	Al/Ni	activity ^b	$M_w^{c,d}$	$M_w/M_n^{c,d}$	$T_m^{e} (°C)$	branches ^f
1	Ni2	20	30	1000	3.45	7.00	34.2	85.5	40
2	Ni2	20	30	1500	3.75	7.35	35.2	84.2	59
3	Ni2	20	30	2000	4.07	6.28	52.0	93.1	46
4	Ni2	20	30	2500	3.56	5.65	38.4	102.3	55
5	Ni2	20	30	3000	2.51	6.15	30.9	103.1	47
6	Ni2	30	30	2000	5.42	6.27	3.6	59.2	69
7	Ni2	40	30	2000	3.81	6.24	6.1	49.7	72
8	Ni2	50	30	2000	2.64	5.20	12.6	46.7	81
9	Ni2	60	30	2000	2.15	3.92	13.6	42.6	98, 220 ^g
10	Ni1	30	30	2000	4.56	7.05	30.1	67.5	57
11	Ni3	30	30	2000	4.34	6.77	64.7	91.5	51
12	Ni4	30	30	2000	5.19	7.73	33.7	73.5	60
13	Ni5	30	30	2000	4.92	7.07	53.9	56.8	68
14	Ni2	30	5	2000	12.36	5.66	14.0	59.9	62
15	Ni2	30	10	2000	6.99	4.70	29.3	61.8	85
16	Ni2	30	20	2000	6.17	5.78	18.3	61.7	50
17	Ni2	30	60	2000	4.03	4.68	31.9	70.7	60
18 ^h	Ni2	30	30	2000	3.31	5.12	30.4	52.2	65
19 ⁱ	Ni2	30	30	2000	0.75	3.21	2.2	30.1	62

^a Conditions: 2 μ mol of Ni; 30 min; total volume 100 ml.

^b $10^6 \text{ g mol}^{-1} (\text{Ni}) \text{ h}^{-1}$.

^c 10^5 g mol^{-1} .

^d determined by GPC.

^e determined by DSC.

^f determined by FT-IR [26].

^g measured by ^{13}C NMR spectroscopy.

^h 5 atm of ethylene.

ⁱ 1 atm of ethylene.

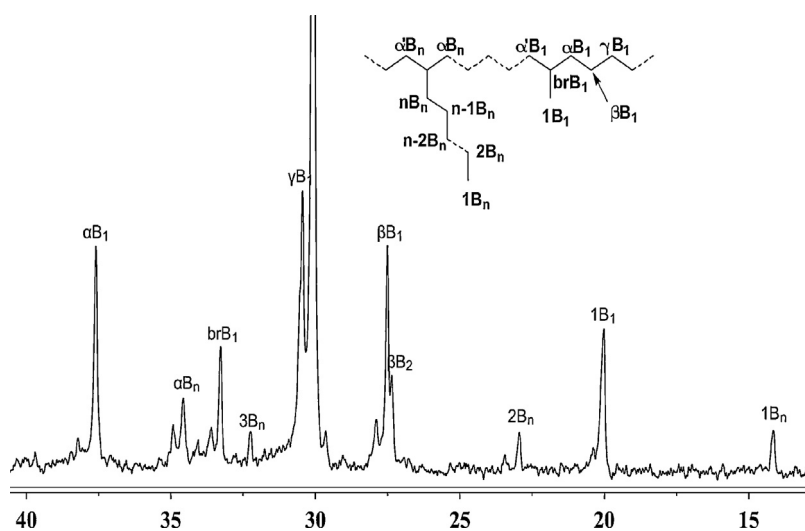


Fig. 7. ^{13}C NMR spectrum of polyethylene by **Ni2/MMAO** at 60°C (run 9, **Table 4**).

distribution. In the presence of MMAO, these precatalysts exhibited high activities for ethylene polymerization (**Table 4**).

In a similar manner, MMAO was also explored with **Ni2** to ascertain the optimum conditions, and the results are tabulated in **Table 4**. Employing the same procedures as for the catalytic system **Ni2/MAO**, the influence of the ratio Al/Ni and reaction temperature on the activities of the **Ni2/MMAO** system indicated that the optimum conditions were 20°C and Al/Ni 2000 (run 6, **Table 4**), which is consistent with **Ni2/MAO**. However, in contrast to the MAO system above, the polyethylene obtained using MMAO as cocatalyst revealed a bimodal molecular weight distribution when the Al/Ni ratio was varied from 1000 to 3000 (as shown in **Fig. 6**). With regard to the influence of the reaction temperature on the PE microstructure (run 3, 6–9, **Table 4**), more branches and lower molecular weight polyethylene were obtained on increasing the temperature. The lower molecular weight at high temperature was attributed to a faster β -hydride elimination rate [12].

In order to assess the branching type in the obtained PE samples, representative polyethylene prepared using **Ni2**-MMAO at 60°C (run 9, **Table 4**) was measured by ^{13}C NMR spectroscopy (**Fig. 7**). According to the method described in the literature [30], it was calculated that polyethylene with 220 branches/1000 carbons was obtained. Highly branched polyethylenes have been also obtained by analogous precatalysts [17] and by aryliminopyridylnickel precatalysts [8–11]. These precatalysts potentially provide alternative processes for solely conducting ethylene polymerization targeting branched polyethylene, which are more commonly produced by the copolymerization of ethylene with α -olefins.

On employing the optimum conditions (Al/Ni = 2000, 30°C over 30 min), the **Ni1–Ni5/MMAO** systems were evaluated for ethylene polymerization (run 6, 10–13, **Table 4**). Different to previous observations [17], it was found here that a bimodal distribution for the polyethylene was obtained using **Ni1**, **Ni3–Ni5/MMAO**, and indicated that more than one kind of active species was operating during the polymerization process when MMAO was used as the cocatalyst. In addition, they showed higher activity for ethylene polymerization than did their corresponding analogs **Ni1’–Ni5’/MMAO** [17]; moreover, the fluorinated systems produced polyethylenes with lower molecular weights. These phenomena are consistent to the above catalytic systems with cocatalyst MAO.

Catalyst lifetimes were also investigated (run 6, 14–15, **Table 4**), and it was observed that the catalytic activities sharply decreased

over 5–10 min (run 14–15, **Table 4**) suggesting that the active species suffered from severe deactivation at reaction times of over 5 min. When the reaction time was prolonged to 60 min, the activity remained fairly constant. However, more polyethylenes of lower molecular weights were obtained on prolonging the time; it is tentatively proposed that the active species present produced the short chain polymers due to difficulties encountered during chain propagation caused by the close presence of the formed polyethylene (and access to less ethylene). The influence of pressure on the ethylene polymerization was also explored. Here also higher molecular weight polymers were obtained at higher ethylene pressure, similar to the result obtained using the Ni-MAO system.

4. Conclusions

A series of unsymmetrical α -diimines nickel(II) complexes (**Ni1–Ni5**) containing the di(Fluorinated benzylhydryl) motif was synthesized and characterized by $^1\text{H}/^{13}\text{C}$ NMR spectroscopy and elemental analysis. When employing either MAO or MMAO as cocatalyst, these complexes exhibited high activity, reaching as high as $10^7 \text{ gPE (mol of Ni)}^{-1} \text{ h}^{-1}$ for ethylene polymerization, producing a bimodal distribution of polymers. The current ligands bearing electron withdrawing fluoro-substituents are capable of inducing net charges in these nickel complexes, and the resulting performance revealed higher activities for ethylene polymerization than observed for their nonfluorinated analogs [17]. These new complexes exhibited much higher activity when using MAO as the cocatalyst. Different to the geometry-constrained acenaphthene-based unsymmetrical α -diimines nickel (II) complexes [14–16], the complexes herein produce polyethylene with a bimodal distribution with either MAO or MMAO as cocatalyst, indicating the potential rotation of the single bond between two imino-groups to generate two active species. Additionally, the polyethylene obtained exhibited a high degree of branching, which was found to vary with temperature.

Acknowledgement

This work is supported by NSFC Nos. 21374123 and U1362204. The RSC and EPSRC are thanked for the awarded of a travel grant (to CR).

Appendix A. Supplementary data

Supplementary data associated with this article can be found, in the online version, at <http://dx.doi.org/10.1016/j.apcata.2014.01.034>.

References

- [1] L.K. Johnson, C.M. Killian, M. Brookhart, *J. Am. Chem. Soc.* 117 (1995) 6414–6415.
- [2] L.K. Johnson, S. Mecking, M. Brookhart, *J. Am. Chem. Soc.* 118 (1996) 267–268.
- [3] S.A. Svejda, M. Brookhart, *Organometallics* 18 (1999) 65–74.
- [4] R. Gao, W.-H. Sun, C. Redshaw, *Catal. Sci. Technol.* 3 (2013) 1172–1179.
- [5] S.D. Ittel, L.K. Johnson, M. Brookhart, *Chem. Rev.* 100 (2000) 1169–1230.
- [6] V.C. Gibson, S.K. Spitzmesser, *Chem. Rev.* 103 (2003) 283–315.
- [7] Z. Guan, C.S. Popeney, *Top Organomet. Chem.* 26 (2009) 179–220.
- [8] S. Wang, W.-H. Sun, C. Redshaw, *J. Organomet. Chem.* 751 (2014) 717–741.
- [9] L. Zhang, E. Yue, B. Liu, P. Serp, C. Redshaw, W.-H. Sun, J. Durand, *Catal. Commun.* 43 (2014) 227–230.
- [10] E. Yue, L. Zhang, Q. Xing, X.-P. Cao, X. Hao, C. Redshaw, W.-H. Sun, *Dalton Trans.* 43 (2014) 423–431.
- [11] E. Yue, Q. Xing, L. Zhang, Q. Shi, X.-P. Cao, L. Wang, C. Redshaw, W.-H. Sun, *Dalton Trans.* 43 (2014) 3339–3346.
- [12] D.P. Gates, S.A. Svejda, E. Onate, C.M. Killian, L.K. Johnson, P.S. White, M. Brookhart, *Macromolecules* 33 (2000) 2320–2334.
- [13] C.M. Killian, L.K. Johnson, M. Brookhart, *Organometallics* 16 (1997) 2005–2007.
- [14] H. Liu, W. Zhao, X. Hao, C. Redshaw, W. Huang, W.-H. Sun, *Organometallics* 30 (2011) 2418–2424.
- [15] H. Liu, W. Zhao, J. Yu, W. Yang, X. Hao, C. Redshaw, L. Chen, W.-H. Sun, *Cata. Sci. Technol.* 2 (2012) 415–422.
- [16] S. Kong, C. Guo, W. Yang, L. Wang, W.-H. Sun, *J. Organomet. Chem.* 725 (2013) 37–45.
- [17] D. Jia, W. Zhang, W. Liu, L. Wang, C. Redshaw, W.-H. Sun, *Cata. Sci. Technol.* 3 (2013) 2737–2745.
- [18] J.L. Rhinehart, L.A. Brown, B.K. Long, *J. Am. Chem. Soc.* 135 (2013) 16316–16319.
- [19] M. Mitani, J. Mohri, Y. Yoshida, J. Saito, S. Ishii, K. Tsuru, S. Matsui, R. Furuyama, T. Nakano, H. Tanaka, S. Kojoh, T. Matsugi, N. Kashiwa, T. Fujita, *J Am Chem Soc.* 124 (2002) 3327–3336.
- [20] D.H. Camacho, E.V. Salo, J.W. Ziller, Z.B. Guan, *Angew. Chem. Int. Ed.* 43 (2004) 1821–1825.
- [21] W.-H. Sun, W. Zhao, J. Yu, W. Zhang, X. Hao, C. Redshaw, *Macromol. Chem. Phys.* (2012) 1266–1273.
- [22] J. Yu, H. Liu, W. Zhang, X. Hao, W.-H. Sun, *Chem. Commun.* 47 (2011) 3257–3259.
- [23] G.M. Sheldrick, *SHELXTL-97, Program for the Refinement of Crystal Structures*, University of Göttingen, Germany, 1997.
- [24] C. Popeney, A. Rheingold, Z.B. Guan, *Organometallics*. 28 (2009) 4452–4463.
- [25] Z.B. Guan, *Chem. Eur. J.* 8 (2002) 3086–3092.
- [26] T. Usami, S. Takayama, *Polym. J.* 16 (1984) 731.
- [27] D. Guo, L. Han, T. Zhang, W.-H. Sun, T. Li, X. Yang, *Macromol. Theory Simul.* 11 (2002) 1006–1012.
- [28] T. Zhang, D. Guo, S. Jie, W.-H. Sun, T. Li, X. Yang, *J. Polym. Sci., Part A: Polym. Chem.* 42 (2004) 4765–4774.
- [29] D.H. Camacho, Z-B. Guan, *Chem. Commun.* 46 (2010) 7879–7893.
- [30] G.B. Galland, R.F. Souza, R.S. Mauler, F.F. Nunes, *Macromolecules* 32 (1999) 1620–1625.